

Original Article

Attenuation correction in single-photon emission computed tomography for NURBS-based cardiac-torso phantom using dual-energy acquisition

ABSTRACT

Single photon emission tomography is widely used to detect photons emitted from the patient. Some of these emitted photons suffer from scattering and absorption because of the attenuation occurred through their path in patient's body. Therefore, the attenuation is the most important problem in single-photon emission computed tomography (SPECT) imaging. Some of the radioisotopes emit gamma rays in different energy levels, and consequently, they have different counts and attenuation coefficients. Calculation of the parameters used in the attenuation equation $N_{out} = \alpha N_{in} = e^{-\mu} N_{in}$ by mathematical methods is useful for the attenuation correction. Nurbs-based cardiac-torso (NCAT) phantom with an adequate attenuation coefficient and activity distribution is used in this study. Simulations were done using SimSET in 20–70 and 20–167 keV. A total of 128 projections were acquired over 360°. The corrected and reference images were compared using a universal image quality index (UIQI). The simulation repeated using NCAT phantom by SimSET. In the first group, no attenuation correction was used, but the Zubal coefficients were used for attenuation correction in the second image group. After the image reconstruction, a comparison between image groups was done using optimized UIQI to determine the quality of used reconstruction methods. Similarities of images were investigated by considering the average sinogram for every block size. The results showed that the proposed method improved the image quality. This study showed that simulation studies are useful tools in the investigation of nuclear medicine researches. We produced a nonattenuated model using Monte Carlo simulation method and compared it with an attenuated model. The proposed reconstruction method improved image resolution and contrast. Regional and general similarities of images could be determined, respectively, from acquired UIQI of small and large block sizes. Resulted curves from both small and large block sizes showed a good similarity between reconstructed and ideal images.

Keywords: Attenuation correction, nurbs-based cardiac-torso phantom, SimSET, single photon emission computed tomography, universal image quality index

INTRODUCTION

The gamma camera is the most important nuclear medicine system, which has made significant advances in this field. For imaging with this camera, the optimum gamma radiation range is 90–200 keV. Photons may interact with orbital electrons, atomic nuclei, or electric fields around them, in which the photon loses a part or whole of its energy. The two types of photoelectric absorption and Compton dispersion occur by passing the photons through the body. In materials with high atomic numbers, photoelectric absorption is more important, but in soft tissues, Compton interactions are more

HOSSEIN RAJABI¹, HADI TALESHI AHANGARI², IRAJ MOHAMMADI^{3,4}, ALIREZA MOHAMMADKARIM², MOHAMMAD ALI TAJIK-MANSOURY²

¹Department of Medical Physics, Faculty of Medical Sciences, Tarbiat Modares University, Tehran, ²Department of Medical Physics, Faculty of Medicine, Semnan University of Medical Sciences, Semnan, ³Department of Basic Sciences, Faculty of Medicine, Sari Branch, Islamic Azad University, Sari, Iran, ⁴Institute of Biophysics and Biomedical Engineering, Faculty of Sciences, University of Lisbon, Lisbon, Portugal


Address for correspondence: Dr. Hadi Taleshi Ahangari, Department of Medical Physics, Faculty of Medicine, Semnan University of Medical Sciences, Semnan, Iran.
E-mail: taleshi@semums.ac.ir

Submission: 17-Jul-19, **Accepted:** 23-Oct-19, **Published:** 22-Aug-20

This is an open access journal, and articles are distributed under the terms of the Creative Commons Attribution-NonCommercial-ShareAlike 4.0 License, which allows others to remix, tweak, and build upon the work non-commercially, as long as appropriate credit is given and the new creations are licensed under the identical terms.

For reprints contact: WKHLRPMedknow_reprints@wolterskluwer.com

How to cite this article: Rajabi H, Ahangari HT, Mohammadi I, Mohammadkarim A, Tajik-Mansoury MA. Attenuation correction in single-photon emission computed tomography for NURBS-based cardiac-torso phantom using dual-energy acquisition. World J Nucl Med 2020;19:211-9.

Access this article online	
Website: www.wjnm.org	Quick Response Code 
DOI: 10.4103/wjnm.WJNM_55_19	

common. Due to attenuation effect, some of the photons scattered or absorbed by the body of the patient are not detected.^[1,2]

One of the most important sources of error in single-photon emission computed tomography (SPECT) images is the intrinsic factor that distort projection data. One of these factors is the attenuation of the beam and the dispersion of radiation in the patient's body. The attenuation causes reconstruction error and changes the image information significantly. A photon must be passed from the patient's body to be a part of a projection. Photoelectric absorption and Compton scattering eliminate the possibility of the presence of photon in one projection. The attenuation problem can be considered as the biggest problem of SPECT imaging.^[3-5]

The photon detection probability depends on the type and length of the organ. According to the Beer's law, the probability of a photon passing through a nonuniform environment is given by the formula of $\alpha = e^{-\mu l}$, where μ is the linear attenuation coefficient and L is the length of the environment. The linear attenuation coefficient shows the probability of absorption or dispersion of a photon in a unit of length (cm^{-1}). In other words, if the number of primary photons is N_{in} , after passing through the thickness of L , the number of photons will be N_{out} .

$$N_{out} = \alpha N_{in} = e^{-\mu L} N_{in} \tag{1}$$

If L is the distance between the place of activity place and the skin surface, it means that L is specified, the above equation can be used to estimate the correct value of the activity inside the patient's body.^[6,7]

The aim of the imaging with gamma camera is to obtain the location and distribution of activity within the patient's body. Therefore, in reconstruction methods, obtaining the depth of activity and the attenuation coefficient of the tissues can be a great help in reconstructing the sinograms. If the depth of activity is not easy to achieve, the geometric mean method is used. To use this method, gamma photons should be counted and recorded in opposite directions, such as anterior and posterior, or left and right views. Assuming that the distance from the activity site to the anterior surface is X_A and to the posterior surface is X_P , the thickness of the body is equal to $L = X_A + X_P$ [Figure 1]. If we show the counting rate of anterior and posterior with I_A and I_P :

$$I_A = N_{in} e^{-\mu X_A} \tag{2}$$

$$I_P = N_{in} e^{-\mu X_P} \tag{3}$$

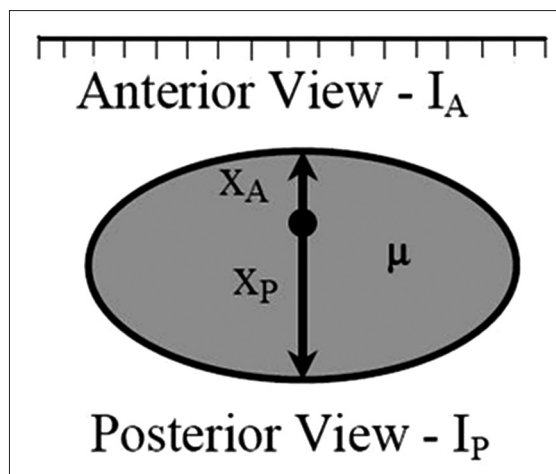


Figure 1: Imaging; the anterior and posterior views of the patient

To calculate the counting rate, N_{in} , the two above equations must be multiplied. As a result, we will have:

$$I_A I_P = N_{in}^2 e^{-\mu(X_A + X_P)} = N_{in}^2 e^{-\mu L} \tag{4}$$

$$N_{in} = \sqrt{(e^{\mu L})} \sqrt{(I_A I_P)} \tag{5}$$

Here, we assume that the attenuation coefficient is uniform, while inside the body, there are materials with a different attenuation coefficient such as bone, fat, muscle, and so on. Another questionable assumption used here was the spotting nature of activity in the patient's body. If the thickness of the organ, where the activity is accumulated in which, in the direction of the gamma camera is W and the distance of the center of the organ to the skin surface of patient is X , we must apply the correction factor of g [Figure 2].

$$I_A = N_{in} g e^{-\mu X} \tag{6}$$

$$I_P = N_{in} g e^{-\mu(L-X)} \tag{7}$$

According to the definition:

$$g = (e^{\eta W/2} - e^{-\eta W/2}) / (\eta W) \tag{8}$$

where η is organ attenuation coefficient, μ is residual effective attenuation coefficient of the body, W is organ width, X is the distance of the center of the organ to the anterior surface, and L is total body thickness.

The standard amount of g in different energies and different materials is available in the nuclear medicine tables.

To correct the attenuation, the thickness and characteristics of the attenuation environment from the radiation source to

the detector must be specified. Therefore, the coordinates of the object and organ must be clearly identified before the reconstruction. There are two general methods for obtaining coordinates. The first method involves ordinary processing. If the imaging is performed in two opposite views (180°), the result of the corrected image depends on the thickness of the object. This method is called the geometric mean method.

$$I_A = N_{in} e^{-\mu x} \tag{9}$$

$$I_P = N_{in} e^{-\mu(L-x)} \tag{10}$$

$$I_{gm} = (I_A I_P)^{\frac{1}{2}} = N_{in} e^{-\mu L/2} \tag{11}$$

N_{in} is the activity of the point source before the attenuation and L is the thickness of the object.

Another method is the use of opposite images and the form of arithmetic mean, which includes depth-dependent variables. The description of this equation is as follows:

$$I_A = N_{in} e^{-\mu x} \tag{12}$$

$$I_P = N_{in} e^{-\mu(L-x)} \tag{13}$$

$$I_{am} = \frac{1}{2} N_{in} \left(e^{-\mu x} + e^{-\mu(L-x)} \right) \tag{14}$$

If the object is centered, it means $x = L - x$, the result, which is similar to the solution obtained from the geometric mean, is as:

$$I_{am} = N_{in} e^{-\mu L/2} \tag{15}$$

In tomography, these images must first be obtained as described and then reconstructed. For nonpoint sources, computation and determination of the coordinates will be very complicated.^[8-12]

For this reason, many efforts have been made to correct the attenuation and different approaches have been proposed so far. The basis of all these methods is the calculation of the attenuation plan of the patient's body. Although each of the proposed methods has been successful to somewhat, the attenuation problem is still not fully solved, and therefore, the use of quantitative methods is difficult in SPECT due to attenuation.^[6-7,13-16]

In this article, it has been tried to introduce a simple, accurate, and rapid method without imposing more absorption dose to the patient. In this study, it has been tried to use the images of multienergy emitter radioisotope to find an attenuation map. For the evaluation of this method, the corrected image

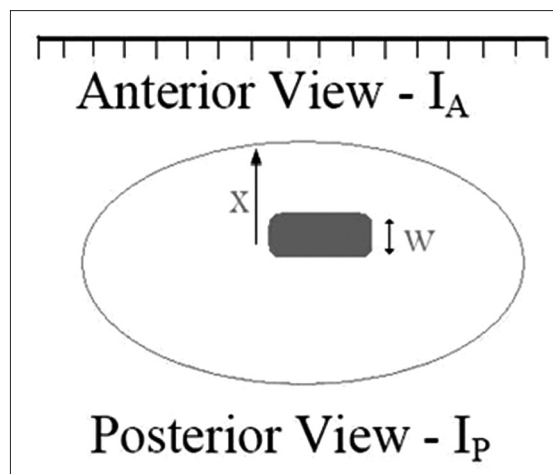


Figure 2: Imaging; thickness of the organ in the anterior and posterior views

was compared with the reference image or original image using the universal image quality index (UIQI).^[17-19]

METHODS

Experimental section

Mathematical description of the studied method

Some radioactive substances emit gamma rays at several levels of energy, and the count and the attenuation coefficient vary at each energy level. On the one hand, in the mean geometric equation, activity, N_{in} , and the attenuation coefficient, μ , are uncertain. Therefore, if we can calculate one of these two variables using equation or other equations, then we can obtain the map of the attenuation coefficient of the texture. The two-element equation of geometric mean can be solved by using these images.

If the count rate of the anterior and posterior images in the first energy level is presented with I_A and I_P , and the count rate of the anterior and posterior images of the second energy level is presented with I'_A and I'_P as the attenuation coefficient is different at each energy level, we have:

$$I_A = N_{in} e^{-\mu_1 X_A} \tag{16}$$

$$I_P = N_{in} e^{-\mu_2 X_P} \tag{17}$$

$$I'_A = \frac{N_{in}}{n} e^{-\mu_1 X_A} \tag{18}$$

$$I'_P = \frac{N_{in}}{n} e^{-\mu_2 X_P} \tag{19}$$

where n is the ratio of photon emission at two levels of energy and is specified. In addition, the numerical value of $X_A + X_P = L$, which is the thickness of the patient's body, is specified. If we show the difference in the level

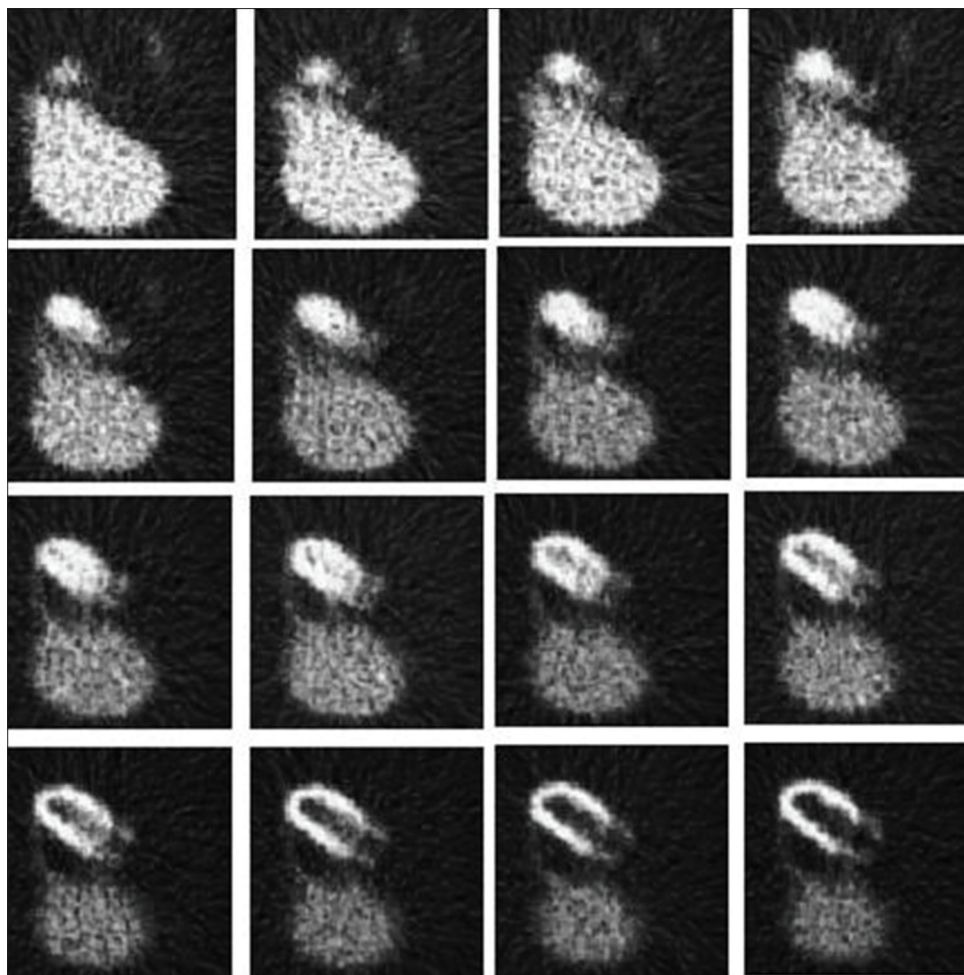


Figure 3: Some reconstructed slices of Tl-201 myocardial perfusion scan without photon attenuation

of the attenuation coefficient of the two energies with a small amount of ϵ , this value can also be extracted from the tables because the attenuation coefficient for different materials and in different energies is well known, so the difference in the attenuation coefficient for two energy levels can be calculated. We have:

$$(\mu'_1 + \mu'_2) - (\mu_1 + \mu_2) = \epsilon \tag{20}$$

Computations required to compensate of the attenuation:

If we multiply the anterior and posterior counts of the first energy level, we have:

$$I_A I_P = N_{in}^2 e^{-\mu_1 X_A - \mu_2 X_P} \tag{21}$$

Moreover, we can multiply the anterior and posterior counts of the second energy level. Therefore, we have:

$$I'_A I'_P = \frac{N_{in}^2}{n^2} e^{-\mu'_1 X_A - \mu'_2 X_P} \tag{22}$$

In the same way, if we divide the anterior and posterior count rates on each other, we have:

$$\frac{I_A}{I_P} = e^{-\mu_1 X_A + \mu_2 X_P} \tag{23}$$

$$\frac{I'_A}{I'_P} = e^{-\mu'_1 X_A + \mu'_2 X_P} \tag{24}$$

Moreover, as a result:

$$\frac{I_A}{I_P} \approx \frac{I'_A}{I'_P} \tag{25}$$

Considering the total count in the anterior and posterior view, we have:

$$I_A + I_P = N_{in} (e^{-\mu_1 X_A} + e^{-\mu_2 X_P}) = N_{in} e^{-\mu_1 X_A} (1 + e^{-\mu_2 X_P + \mu_1 X_A}) \tag{26}$$

$$= N_{in} e^{-\mu_2 X_P} (1 + e^{-\mu_1 X_A + \mu_2 X_P})$$

$$I'_A + I'_P = \frac{N_{in}}{n} (e^{-\mu'_1 X_A} + e^{-\mu'_2 X_P}) = \frac{N_{in}}{n} e^{-\mu'_1 X_A} (1 + e^{-\mu'_2 X_P + \mu'_1 X_A}) \tag{27}$$

$$= \frac{N_{in}}{n} e^{-\mu'_2 X_P} (1 + e^{-\mu'_1 X_A + \mu'_2 X_P})$$

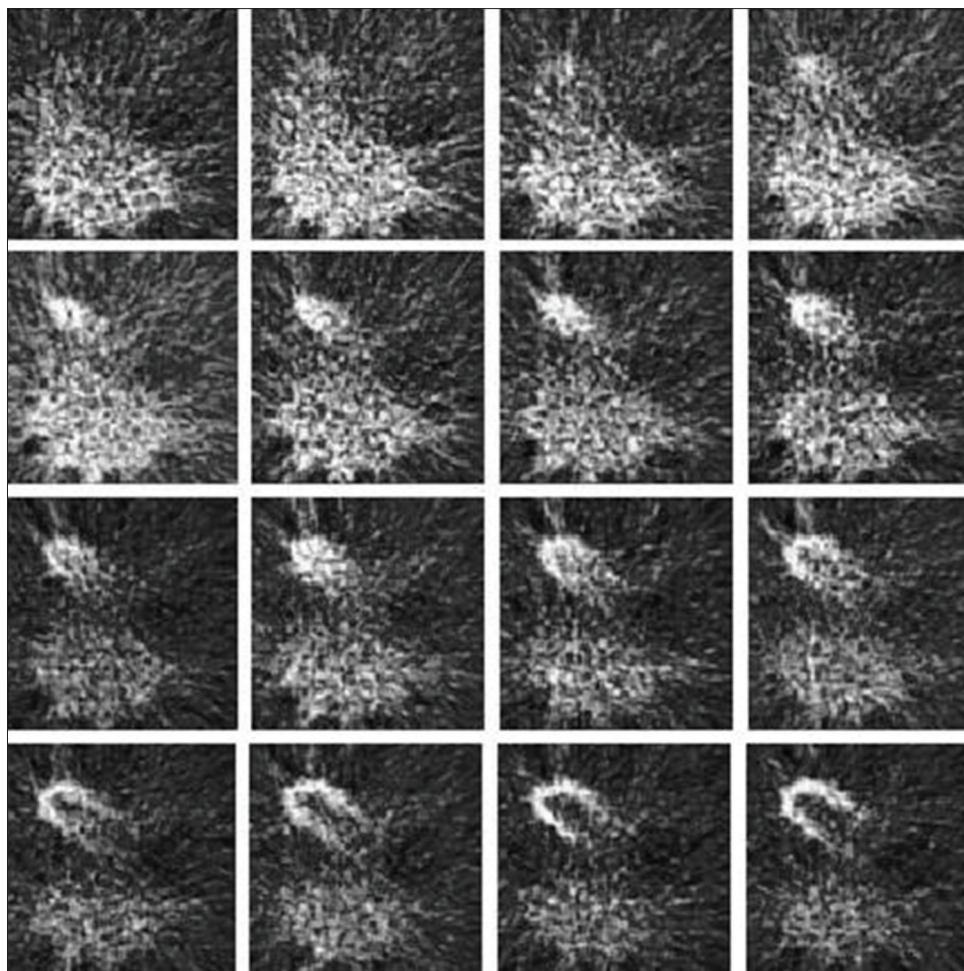


Figure 4: Some reconstructed slices of Tl-201 myocardial perfusion scan with photon attenuation, without attenuation correction

By dividing the pairwise equations of the views in two energies, we have:

$$\frac{I_A I_p}{I'_A I'_p} = \frac{e^{-\mu_1 X_A - \mu_2 X_p}}{e^{-\mu'_1 X_A - \mu'_2 X_p}} = n^2 e^{(\mu'_1 - \mu_1) X_A + (\mu'_2 - \mu_2) X_p} = n^2 e^{\epsilon L} \quad (28)$$

The above equation is assumed to be linear in the attenuation coefficient in two energies. Considering the total count in the anterior and posterior view, we have:

$$\frac{(I_A + I_p)}{(I'_A + I'_p)} = \frac{ne^{-\mu_2 X_p} (1 + e^{-\mu_1 X_A + \mu_2 X_p})}{e^{-\mu'_2 X_p} (1 + e^{-\mu'_1 X_A + \mu'_2 X_p})} \approx \frac{ne^{-\mu_2 X_p}}{e^{-\mu'_2 X_p}} \cdot \frac{\left(1 + \frac{I_A}{I_p}\right)}{\left(1 + \frac{I'_A}{I'_p}\right)} = ne^{\epsilon X_p} \quad (29)$$

$$\frac{I_A I_p (I_A + I_p)}{I'_A I'_p (I'_A + I'_p)} = ne^{\epsilon L - \epsilon X_p} \approx ne^{\epsilon X_A} \quad (30)$$

To compensate the attenuation completely, the number of counts counted must be multiplied in $e^{\mu X_p}$. The equation of $e^{\epsilon X_p}$

is not exactly equal to $e^{\mu X_p}$ but it can compensate the photons attenuation inside the patient's body to an acceptable level. As a result, the final equation to be reconstructed based on it is as follows:

$$nI_A \frac{I_A I_p (I_A + I_p)}{I'_A I'_p (I'_A + I'_p)} \approx I_0 \quad (31)$$

where I_0 is the actual activity in the patient's body.

Method validation

The nurbs-based cardiac-torso (NCAT) phantom, which is a three-dimensional analytical phantom and generates a realistic attenuation coefficient and activity distributions inside the chest, has been used. This activity distribution was investigated for two levels of energy. The simulation was performed using SimSET simulator in the energies of 70 and 167 keV by assuming a Tl-201 tracer at concentrations of 75, 2, and 4 in the heart, lung, and soft tissues, respectively, and taking into account, the attenuation coefficient for bone, lungs, and muscle in the energy. The radiation source and the attenuation map were

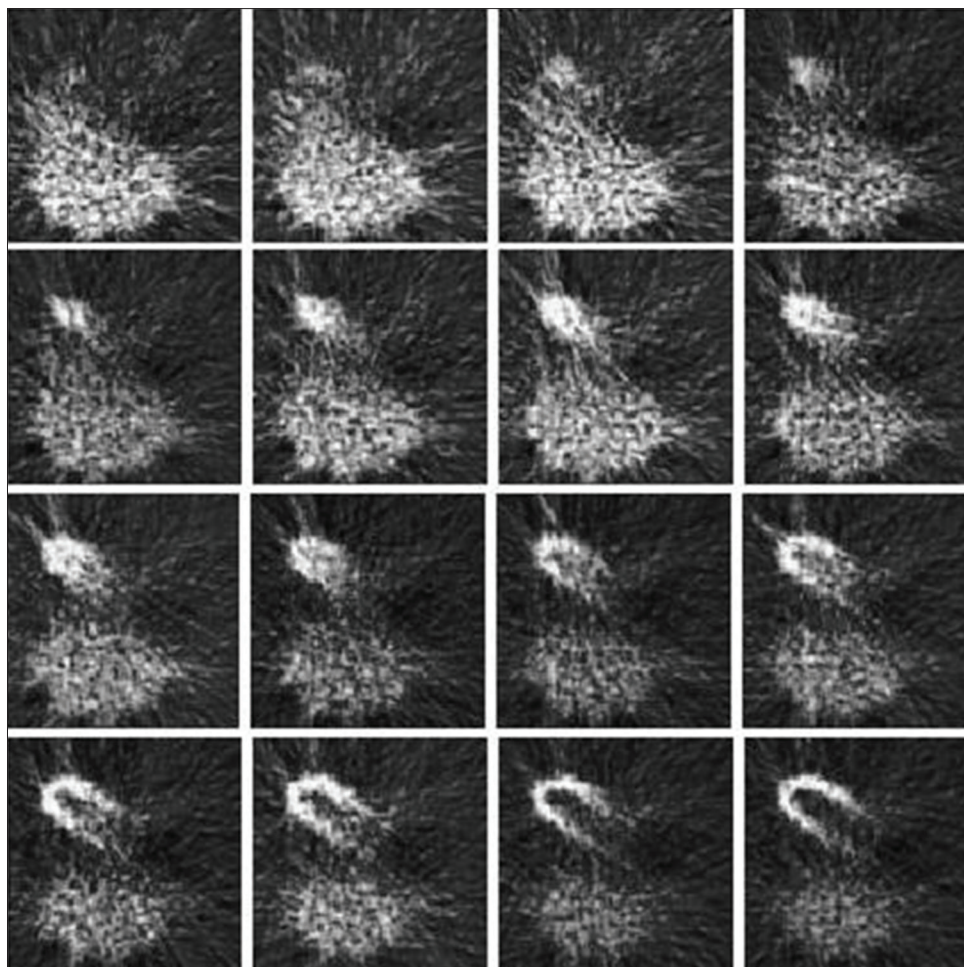


Figure 5: Some reconstructed slices of Tl-201 myocardial perfusion scan with photon attenuation, with attenuation correction using the proposed method

divided into 128×128 pixels with a size of each pixel of 3.75×3.75 mm. The collimator was considered as a complete parallel-hole collimator, and the signal-to-noise ratio was considered according to Poisson noise. For all simulations, 10^7 photons were considered to assure statistical uncertainty of below 5%. One hundred and twenty-eight projections were made at 360° in an energy window of $\pm 20\%$. The optimized UIQI parameter was used as a comparison criterion for the used sinograms to show the similarity of the actual attenuation map with the obtained attenuation map.^[20-22]

RESULTS

Initially, two similar simulations were performed with the NCAT phantom and SimSET simulator [Figure 3]. The first simulation was performed without applying the attenuation coefficient, and in the second simulation, which was the repetition of the first simulation, the Zubal coefficients were used as an attenuation model and photons related to the energy window of 167 keV were recorded [Figure 4].

In order to compare and evaluate the images, the sinograms simulated with the second simulation were reconstructed using the proposed method [Figure 5].

After reconstructing, the optimized UIQI parameter was used to compare the images in a nonattenuation state to determine the similarity of each reconstruction method with the original image [Figure 6]. Therefore, the similarity of the images was evaluated [Figure 7].

DISCUSSION

For photons to be counted, they must, of course, pass through the patient's body and reach the detectors. Photoelectric absorption and Compton's scattering eliminate photon's presence in a single view. Therefore, the attenuated views include fewer events than the ideal state. The possibility of photon detection depends on the type and length of the organ. Linear attenuation coefficient shows the probability of absorbing or dispersing a photon per unit length. It can be said that the attenuation is the biggest problem with SPECT imaging.

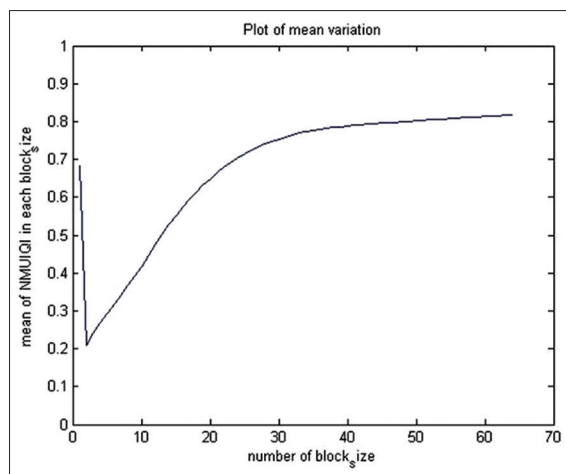


Figure 6: The similarity of the reconstructed slices of TI-201 myocardial perfusion scan between images without photon attenuation and with photon attenuation without attenuation correction

The aim of the imaging with the gamma camera is to obtain the location and distribution of activity within the patient's body. Therefore, in reconstruction methods, obtaining the depth of activity and the coefficient of attenuation of the tissues can be a great help in reconstructing the sinograms.

The geometric mean method is one of the methods currently used to obtain the depth of activity. To use this method, counts should be recorded in opposite directions. It is assumed with the assumption of uniformity of the attenuation coefficient, while inside the body there are materials with a different coefficient of attenuation. Another method is the use of opposite images and arithmetic mean form, which includes depth-dependent variables. Although each of the proposed methods has been somewhat successful, the attenuation problem is still not fully solved, and therefore, due to attenuation, the use of quantitative methods in SPECT is difficult.^[14-15,23]

Anyway, in each direction, an attenuation factor can be considered which the counting reduced as well. If this coefficient of attenuation can be achieved or even close to a certain extent, we will be able to increase the counts in the detector and thereby reduce the noise of the background or reconstruction and improve the contrast. This amount of attenuation coefficient is different in the two sides of the ray of radiopharmaceutical because of the difference in body tissues coefficient and their thickness. Furthermore, there may be different attenuation in two detectors that are simultaneously counting the gamma rays at the two sides of the body. In addition, some radioactive substances emit several levels of gamma-ray energy and the amount of counting and the attenuation coefficient vary at each energy level.^[23-25]

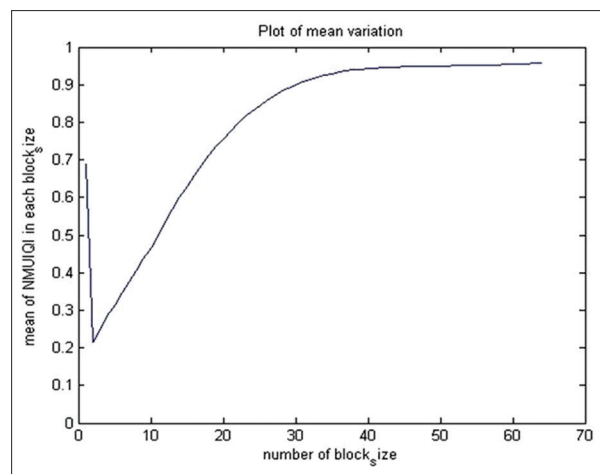


Figure 7: Similarity of the reconstructed slices of TI-201 myocardial perfusion scan between images without photon attenuation and with photon attenuation with attenuation correction using the proposed method

The difference between the number of counts and the difference in energy level can be used to calculate the attenuation plan. The calculation is done by considering the difference in counting in pixels with the assumption of linearity of the attenuation coefficient. Using simulation, a study can be done at the lowest cost without requiring a patient test or imposing an additional dose. In some experiments, the cost or dangers are so high that you cannot decide on that. Even there is not too much hope in animal models or phantoms. In some cases, it is necessary to conduct experiments in an ideal state and to remove or influence a particular parameter. Simulation enables the experiments to be done with the least difficulty.

Attenuation correction procedure by using dual-energy acquisition technique was previously reported for circularly symmetric phantom of the head region.^[26] In this study, due to the problems and parameters of the research, it was necessary to simulate with special capabilities for imaging and performing calculations. For this reason, the NCAT phantom, a phantom almost equivalent to the human body, was used as a phantom in SimSET simulation code.^[20-22]

In this research, via Monte Carlo simulator model, a model was created in the presence of attenuation factors, and after mathematical calculation and reconstruction, we compared this model with the model which was created without attenuation coefficient. As expected, gamma rays are scattered by attenuation. Furthermore, a lower count is reached on the detector, and as a result, the image from the reconstruction has a higher noise and less contrast than the nonattenuation one. To obtain the formulas, we could not reach the final formula directly and without any experiment. Hence, step by step at each stage, we arrived at

a new stage by obtaining the formula and writing a program in MATLAB software and doing the reconstruction. TI-201 is the most common available and used radioactive isotope in treatment centers and hospitals that has two levels of energy. Therefore, due to the availability and relatively easy use of this radiopharmaceutical, simulations were carried out in accordance with the energy levels of this radiopharmaceutical.

To evaluate the images, they can be quantitatively and qualitatively analyzed. Visual examination depends on the skill and nature of the images, and so can only be cited in a simple and specific condition where the difference between the two images is obvious. As a result, in this research, we could not use the high volume of images and a slight reduction in the quality. Undoubtedly, the authenticity and method of the comparison could have played a fundamental role about the success rate of the processing method.

The comparison methods of the statistical indicators which currently used to compare nuclear medical images do not provide acceptable results. The main reason for this is the lack of high noise and low ratio of signal to noise in nuclear medical images. These indicators are highly influenced by the noise of the images, so that small differences between images disappear in the random statistical difference of the noise. Therefore, the sensitivity of these methods is negligible to determine the small differences between the images. Therefore, UIQI index was suggested to solve these problems. The UIQI index shows the difference in local error in the small size block, and in the larger size block, it expresses the general and overall difference error of the image. For this reason, we could use this parameter with slight changes in this index and optimize it.^[18]

As the UIQI optimized parameter indicates, there was no difference in the lower-level block between the charts. However, with the increasing of the block, the size difference between the two graphs increased too. This meant that the background count or noise had reduced in the proposed method; as a result, the contrast of the image is increased. In the simulation environment, the improvement of the quality of the proposed method is more acceptable than the usual methods of reconstruction. Therefore, it can be used as a method to reconstruct the image in later stages.

CONCLUSION

Application of simulator software causes to largely overcome the problems of research in this field of nuclear medicine imaging. In this study, using Monte Carlo simulator code,

SPECT data were acquired with and without applying attenuation correction and then, after reconstruction, images were compared. As expected, gamma rays are scattered by attenuating. Moreover, less counts reach to the detector, and as a result, the image resulted from the reconstruction has more noise and less contrast than that resulted by the nonattenuation mode.

In the reconstruction with the proposed method, the resolution and contrast of the images were improved, and the number of calculated counts was closer to the number of counts of the first simulation. The comparison of the optimized UIQI parameter shows that the similarity and number of reconstruction counts in different block sizes have been significantly increased using the proposed method. In low block sizes, the UIQI parameter determines the regional similarity of two images, and in higher block sizes, it determines the overall similarity of two images. The obtained graphs, both in the small block sizes and in the large block sizes, show more similarity of the reconstructed image and the proposed method with the ideal state.

Financial support and sponsorship

This study was supported by a grant from Tarbiat Modares University.

Conflicts of interest

There are no conflicts of interest.

REFERENCES

1. Saha GB. *Physics and Radiobiology of Nuclear Medicine*. New York, USA: Springer Science and Business Media; 2013.
2. Knoll P, Rahmim A, Gültekin S, Šamal M, Ljungberg M, Mirzaei S, *et al.* Improved scatter correction with factor analysis for planar and SPECT imaging. *Rev Sci Instrum* 2017;88:094303:1-10.
3. Berker Y, Li Y. Attenuation correction in emission tomography using the emission data – A review. *Med Phys* 2016;43:807-32.
4. Gourion D, Noll D, Gantet P, Esquerré JP. Attenuation correction using SPECT emission data only. *IEEE Trans. Nucl Sci* 2002;49:2172-9.
5. Hutton BF, Buvat I, Beekman FJ. Review and current status of SPECT scatter correction. *Phys Med Biol* 2011;56:R85-112.
6. Zaidi H, Hasegawa B. Determination of the attenuation map in emission tomography. *J Nucl Med* 2003;44:291-315.
7. King M, Farncombe T. An overview of attenuation and scatter correction of planar and SPECT data for dosimetry studies. *Cancer Biother Radiopharm* 2003;18:181-90.
8. Sadrmomtaz A, Kakasoltani S. Scatter correction with dual energy window method in SPECT and investigation the effect of scatter correction on image contrast value in reconstructed data. *World Appl Program* 2011;1:150-4.
9. Alfuraih A, Kadri O, Alzimami K. Investigation of SPECT/CT cardiac imaging using Geant4. *Nucl Sci Tech* 2018;29:105.
10. Mohammadi I, Rajabi H, Pouladian M, Sadeghi M, Shirazi A. Detection and evaluation of patient motion in myocardial SPECT imaging using modeling of projections by polynomial curves and 2D curve fitting. *U.P.B Sci Bull Series A* 2014;76:63-76.

11. Ficarò EP, Fessler JA, Rogers WL, Schwaiger M. Comparison of americium-241 and technetium-99m as transmission sources for attenuation correction of thallium-201 SPECT imaging of the heart. *J Nucl Med* 1994;35:652-63.
12. Capote RM, Matela N, Conceição RC, Almeida P. Optimization of convergent collimators for pixelated SPECT systems. *Med Phys* 2013;40:062501:1-13.
13. Yamauchi Y, Kanzaki Y, Hayashi M, Arai M, Morita H, Komori T, *et al.* Improved diagnosis of the number of stenosed coronary artery vessels by segmentation with scatter and photo-peak window data for attenuation correction in myocardial perfusion SPECT. *J Nucl Cardiol* 2019;26:574-81.
14. Mennessier C, Noo F, Clackdoyle R, Bal G, Desbat L. Attenuation correction in SPECT using consistency conditions for the exponential ray transform. *Phys Med Biol* 1999;44:2483-510.
15. Yan Y, Zeng GL. Attenuation map estimation with SPECT emission data only. *Int J Imaging Syst Technol* 2009;19:271.
16. Ermis EE, Pilicer FB, Pilicer E, Celiktas C. A comprehensive study for mass attenuation coefficients of different parts of the human body through Monte Carlo methods. *Nucl Sci Tech* 2016;27:54.
17. Wang Z, Bovik AC, Lu L. Why is Image Quality Assessment so Difficult? Acoustics, Speech, and Signal Processing, 2002. Proceedings. (ICASSP '02). IEEE International Conference on Acoustics, Speech, and Signal Processing, Proceedings. Vol. 4; 2002.
18. Wang Z, Bovik AC. A universal image quality index. *IEEE Signal Process Lett* 2002;9:81-4.
19. Raeisi E, Rajabi H, Aghamiri S. A new approach for quantitative evaluation of reconstruction algorithms in SPECT. *Int J Radiat Res* 2006;4:77-80.
20. Segars W, Tsui B, Lalush D. Development and application of the new dynamic nurbs-based cardiac-torso (NCAT) phantom. *J Nucl Med* 2001;42:23.
21. Zubal IG, Harrell CR, Smith EO, Rattner Z, Gindi G, Hoffer PB, *et al.* Computerized three-dimensional segmented human anatomy. *Med Phys* 1994;21:299-302.
22. Haynor DR, Harrison RL, Lewellen TK. The use of importance sampling techniques to improve the efficiency of photon tracking in emission tomography simulations. *Med Phys* 1991;18:990-1001.
23. Tavakoli M, Naji M, Abdollahi A, Kalantari F. Attenuation Correction in SPECT Images Using Attenuation map Estimation with its Emission data. *Proceedings, Physics of Medical Imaging*. Vol. 10132; 2017.
24. Takeuchi W, Suzuki A, Shiga T, Kubo N, Morimoto Y, Ueno Y, *et al.* Simultaneous tc-99m and I-123 dual-radionuclide imaging with a solid-state detector-based brain-SPECT system and energy-based scatter correction. *EJNMMI Phys* 2016;3:10.
25. Danad I, Fayad ZA, Willeminck MJ, Min JK. New applications of cardiac computed tomography: Dual-energy, spectral, and molecular CT imaging. *JACC Cardiovasc Imaging* 2015;8:710-23.
26. Nalcioğlu O, Bor D. Dual energy attenuation correction for single photon emission computed tomography (SPECT). *IEEE Trans Nucl Sci* 2015;31:590-3.